Cancer Cell
Article

Coordinated Silencing of MYC-Mediated miR-29 by HDAC3 and EZH2 as a Therapeutic Target of Histone Modification in Aggressive B-Cell Lymphomas

Xinwei Zhang,[1,4,10] Xiaohong Zhao,[1,10] Warren Fiskus,[5] Jianhong Lin,[6] Tint Lwin,[1] Rekha Rao,[5] Yizhuo Zhang,[4] John C. Chan,[7] Kai Fu,[7] Victor E. Marquez,[8] Selina Chen-Kiang,[9] Lynn C. Moscinski,[1] Edward Seto,[2] William S. Dalton,[1] Kenneth L. Wright,[3] Eduardo Sotomayor,[1] Kapil Bhalla,[5] and Jianguo Tao[1,*]

[1]Department of Malignant Hematology and Experimental Therapeutics Program
[2]Molecular Oncology Program
[3]Immunology Program
H. Lee Moffitt Cancer Center and Research Institute, Tampa, FL 33613, USA
[4]Department of Immunology and Malignant Hematology, Tianjin Cancer Hospital, Tianjin 300060, China
[5]The Drug Discovery, Delivery and Experimental Therapeutics, University of Kansas Cancer Center, Kansas City, KS 66160, USA
[6]Dana-Farber Cancer Institute, Boston, MA 02115, USA
[7]Department of Pathology, University of Nebraska Medical Center, Omaha, NE 68198, USA
[8]Chemical Biology Laboratory, Center for Cancer Research, National Cancer Institute, Frederick, MD 21702, USA
[9]Department of Pathology, Weill-Cornell Medical College, New York, NY 10065, USA
[10]These authors contributed equally to this work
*Correspondence: jianguo.tao@moffitt.org
http://dx.doi.org/10.1016/j.ccr.2012.09.003

SUMMARY

We investigated the transcriptional and epigenetic repression of miR-29 by *MYC*, *HDAC3*, and *EZH2* in mantle cell lymphoma and other *MYC*-associated lymphomas. We demonstrate that miR-29 is repressed by MYC through a corepressor complex with HDAC3 and EZH2. MYC contributes to EZH2 upregulation via repression of the EZH2 targeting miR-26a, and EZH2 induces MYC via inhibition of the MYC targeting miR-494 to create positive feedback. Combined inhibition of HDAC3 and EZH2 cooperatively disrupted the MYC-EZH2-miR-29 axis, resulting in restoration of miR-29 expression, downregulation of miR-29-targeted genes, and lymphoma growth suppression in vitro and in vivo. These findings define a MYC-mediated miRNA repression mechanism, shed light on *MYC* lymphomagenesis mechanisms, and reveal promising therapeutic targets for aggressive B-cell malignancies.

INTRODUCTION

c-MYC (hereinafter termed MYC) is a transcription factor that promotes oncogenesis by activating and repressing its target genes that control cell growth and proliferation (Nilsson and Cleveland, 2003). MYC is deregulated in a large proportion of aggressive B-cell lymphomas. Although MYC has been described as a defining feature and the driving oncogene for Burkitt lymphoma, the significance of MYC has also been recognized in other non-Hodgkin's lymphomas (Dave et al., 2006). MYC, which has been detected in 9%–14% of diffuse large B-cell lymphomas, is associated with an adverse prognosis as a result of chemoresistance and with shortened survival. In mantle cell lymphoma (MCL), increased expression of MYC has been found to be associated with poor prognosis and MCL aggressiveness (Hartmann et al., 2008). MYC overexpression has been implicated in high-grade large cell transformation in follicular and marginal zone cell lymphomas (Slack and

Significance

Aberrant miRNA expression and miRNA oncogenic and tumor suppressive functions have been extensively investigated in many tumors, including lymphoma; however, the molecular basis for miRNA dysregulation remains unknown and emerging. Our findings of miRNA regulation by c-MYC (hereafter termed MYC) and epigenetic deacetylation by HDAC3 and trimethylation by EZH2 present a common mechanism for repression of many other tumor suppressor miRNAs. We demonstrated a MYC-miRNA-EZH2 feed-forward pathway that leads to persistent MYC and EZH2 overexpression and miR-29 repression, thus maintaining tumorigenic potential of lymphoma cells. Restoration of miR-29 expression through epigenetic drug cotreatment resulted in enhanced inhibition of oncogenic signaling pathways, lymphoma growth in vivo, and is a therapeutic target of histone modifications in aggressive B-cell lymphomas.

Gascoyne, 2011), supporting the features of MYC in sustaining aggressive transformation of lymphomas. Despite current modes of intensive chemotherapy and radiation, survival in patients with high MYC activity is dismal. It is still unclear what direct MYC-induced transcriptional changes promote cell transformation, and the therapeutics against MYC has remained elusive.

Aberrant micro-RNA (miRNA) expression and miRNA oncogenic and tumor suppressive functions have been extensively investigated in many tumors, including lymphomas (Fabbri and Croce, 2011). However, the molecular basis for miRNA dysregulation remains uncharacterized and emerging (Liu et al., 2010). Our work and that of others have indicated that the *miR-29* family might function as a tumor suppressor (Fabbri et al., 2007; Zhao et al., 2010). Expression of these miRNAs inhibits cell proliferation, promotes apoptosis of cancer cells, and suppresses tumorigenicity by targeting multiple oncogenes. Loss or downregulation of these miRNAs has been reported in a variety of hematopoietic and solid tumors and has been shown to be associated with high-risk chronic lymphocytic leukemia, lung cancer, invasive breast cancer, and cholangiocarcinoma (Fabbri and Croce, 2011). These observations are consistent with our recent study demonstrating that miR-29 is downregulated in aggressive MCL (Zhao et al., 2010).

MYC has been recently implicated in controlling the expression of a host of miRNAs (Chang et al., 2008). The predominant consequence of activation of MYC is widespread repression of miRNA expression. Although the mechanisms by which MYC activates transcription have been extensively studied, less is known about how MYC represses transcription of target genes as well as miRNAs. It was reported that MYC repressed target genes *Id2* and *Gadd153* by recruitment of *histone deacetylase 3* (*HDAC3*) (Kurland and Tansey, 2008). More recently, our study demonstrated that MYC acts as a repressor of miRNA-15a/16 by recruiting HDAC3 (Zhang et al., 2012). These findings suggest that histone deacetylation may be involved in MYC-mediated transcriptional repression. Further evidence has shown that histone H3 lysine 27 trimethylation, which is mediated by *enhancer of zeste homolog 2* (*EZH2*) at the promoter of the gene, leads to silencing of gene expression (Chen et al., 2005). The polycomb-repressive complex 2 (PRC2) contains three core proteins (EZH2, SUZ12, and EED), and PRC2 is a transcriptional repressor that has a crucial function in maintaining the delicate homeostatic balance between gene expression and repression, the disruption of which may lead to oncogenesis (Sparmann and van Lohuizen, 2006). The roles of HDAC and PRC2 in miRNA regulation and dysregulation are largely unknown and have been poorly defined so far.

In this study, we explored the role of MYC, HDAC, and EZH2 in miR-29 repression and the contribution of miR-29 to cell survival and growth in MYC-associated lymphomas. We examined the regulation and functional roles of miRNAs, histone modifications and their interplay in MYC, EZH2 overexpression, and the tumorigenic potential of lymphoma cells. Furthermore, we tested molecular targeting strategies to restore miR-29 expression and examined whether combined inhibitors of HDAC and EZH2 cooperatively increase miR-29 expression and inhibit lymphoma growth and shorten in vivo lymphoma survival.

RESULTS

MYC Is Overexpressed in Aggressive MCL and Is Inversely Correlated with Expression of miR-29

We examined MYC and miR-29 expression and their correlation using purified lymphoma cells from MCL patients and normal donors. As shown in Figure 1A, compared with normal $CD19^+$ peripheral blood lymphocytes, miR-29a-c was significantly downregulated and MYC was significantly overexpressed in MCL samples. Furthermore, MCLs with higher MYC expression have significantly lower miR-29 expression. We used the P493-6 human B-cell line as a model to examine the role of MYC in miR-29 expression. P493-6 cells bear a tetracycline (tet)-repressible MYC construct such that tet withdrawal results in rapid induction of MYC followed by cell proliferation. We compared expression levels of MYC and miR-29 in tet-treated (MYC-off) and untreated (MYC-on) cells and observed an inverse correlation between miR-29 and MYC expression (Figures 1B–1D). Expression of primary miR-29 (pri-miR-29a/b1 and pri-miR-29b2/c) and mature miR-29 was measured by quantitative reverse-transcribed polymerase chain reaction (qRT-PCR) in P493-6 cells with and without MYC expression. We found both primary miR-29 and mature miR-29 to be remarkably lower in MYC-on B cells than in MYC-off cells, whereas MYC repression after tet treatment significantly upregulated, miR29a-c. In addition, MCL patient samples showed strong positive correlations between primary miRNAs of miR-29 and mature miR-29 expression (Figures S1A–S1C available online).

MYC, HDAC3, and PRC2 Are Tethered to the miR-29 Promoter Regions as a Corepressor Complex to Downregulate miR-29 Expression through Histone Deacetylation and Trimethylation

We next investigated the epigenetic regulation of MYC-induced miR-29 repression through histone acetylation and methylation. We first examined the effects of chromatin-modifying drugs on miR-29 expression in MCL and other MYC-expressing B-cell lymphomas. Using qRT-PCR, we evaluated the effects of a pan-HDAC inhibitor (vorinostat) on both primary and mature miR-29 expression in MCL (Jeko-1) and Burkitt lymphoma cells (Ramos). Figure 2A shows that vorinostat caused a dose-dependent increase in miR-29a-c expression. miR-29 induction was also observed with another HDAC inhibitor, trichostatin A (Figure S2A), suggesting an HDAC role in miR-29 gene expression and supporting that the miR-29 family members are subject to epigenetic control in lymphoma cells. We next studied the role of PRC2 in the downregulation of miR-29 since PRC2 has been shown to be recruited to gene promoters to induce histone trimethylation and gene repression. We evaluated the effects of the PRC2 inhibitor 3-deazaneplanocin A (DZNep) on miR-29 expression. Based on our previous study of using DZNep for leukemia cells (Fiskus et al., 2009), we chose the DZNep dosage range and revealed that DZNep resultes in a dose-dependent decrease in the protein expression of EZH2 and SUZ12 (Figure 2B; Figure S2B) and caused a dose-dependent increase in pri-miR-29a/b1, pri-miR-29b2/c, and mature miR-29 expression in these lymphoma cell lines (Figure 2C; Figure S2C). Overall, the above observations implied that both HDAC and PRC2 are involved in miR-29 expression.

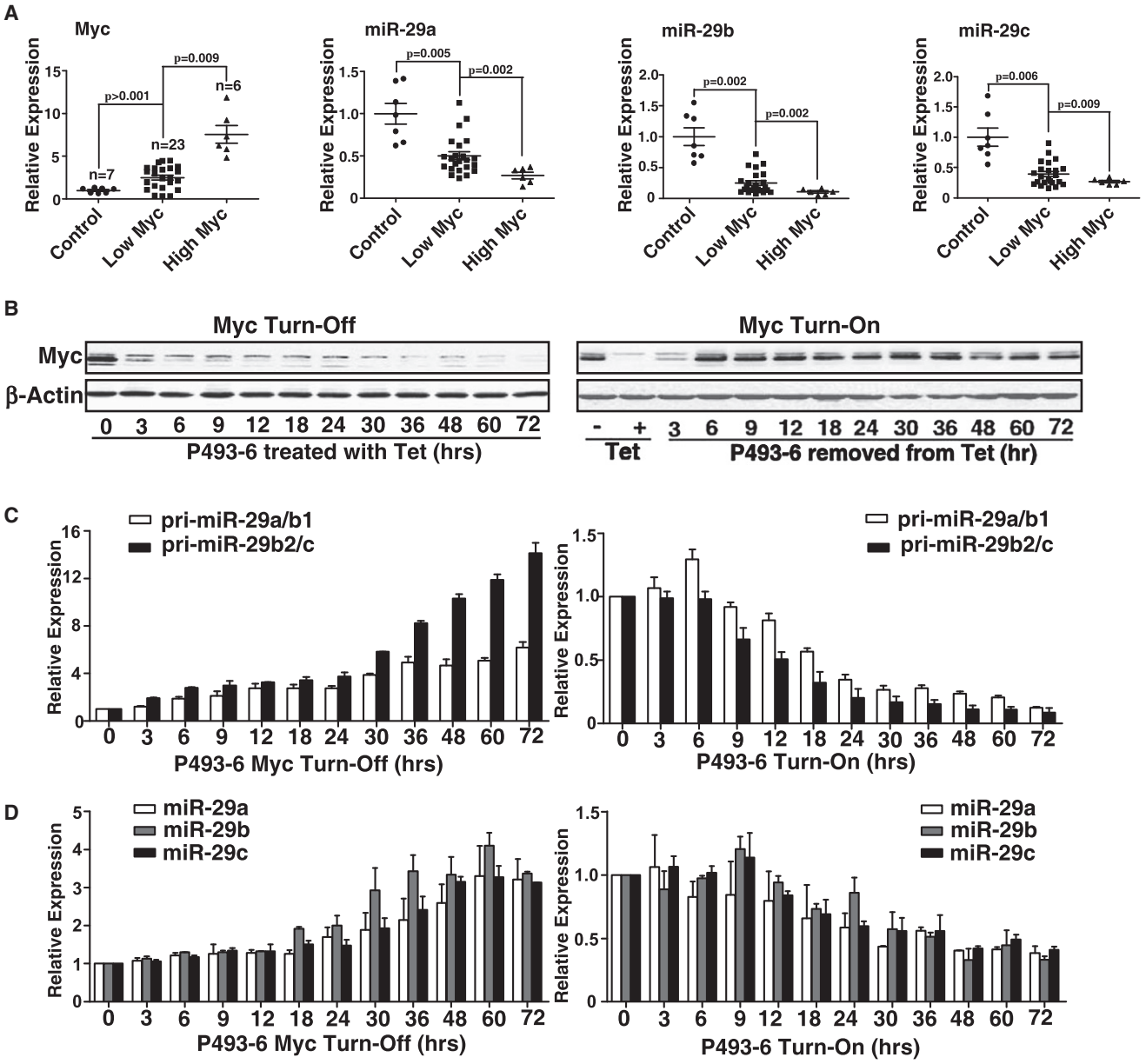

Figure 1. MYC Is Overexpressed in Aggressive MCLs and Is Inversely Correlated with Expression of miR-29

(A) miR-29a-c expression inversely correlated with MYC expression in primary MCL cells. Expression levels of miR-29a-c and MYC in normal B lymphocytes and primary MCL samples were measured by qRT-PCR. The high MYC group is defined as those samples in the upper quartile (25%) of MYC expression, while all others are placed in the low MYC group for the patient samples.

(B–D) Expression of MYC and miR29a-c in tet-treated (MYC turn-off or MYC-off) and untreated (MYC turn-on or MYC-on) P493-6 cells. (B) Western blot shows MYC expression levels in MYC-off P493-6 cells treated with tet and in MYC-on P493-6 cells after removal of tet for indicated times. (C) Pri-miR-29 expression levels in MYC-off P493-6 cells treated with tet and in MYC-on P493-6 cells after removal of tet for indicated times. (D) Mature miR-29 and MYC expression levels in MYC-off P493-6 cells treated with tet and in MYC-on P493-6 cells after removal of tet for indicated times. Pri-miR-29 level was normalized to GAPDH, and mature miR-29 expression was normalized to RNU44. Results in (B) are representative of three independent experiments. Results in (C) and (D) are means ± SD from at least three biological replicates.

See also Figure S1.

We explored whether MYC, HDAC3, and/or EZH2 act together to be involved in miR-29 expression in MYC-expressing lymphoma cells. The role of MYC and HDAC3 in the transcriptional regulation of miR-29 gene expression was first examined by depleting the expression of MYC and HDAC3, respectively, with siRNA. Expression levels of primary and mature miR-29 were analyzed after MYC or HDAC3 was knocked down. In agreement with our earlier results with vorinostat, knockdown of HDAC3 significantly enhanced both primary and mature miR-29 gene expression (Figure 2D). Moreover, knockdown of

MYC also markedly increased miR-29 gene expression and decreased EZH2 expression (Figure 2D). When we assessed the role of PRC2 in MYC-mediated miR-29 repression, we found that depletion of EZH2 and/or SUZ12 using siRNAs also significantly increased miR-29 gene expression and decreased MYC expression (Figure 2E), further supporting the role of EZH2/PRC2 in miR-29 expression.

Next, we examined the miR-29a/b1 and miR-29b2/c gene promoter regions for transcription factor binding sites and identified three highly conserved MYC binding sites—S1, S2, and S3—in a region ~5 kb upstream and in the first intron of both human miR-29a/b1 and miR-29b2/c (Figure 3A). We investigated whether HDAC3 and EZH2/PRC2 could be recruited to the miR-29 promoters by MYC and whether HDAC3 and EZH2 mediated MYC-induced miR-29 repression using chromatin immunoprecipitation (ChIP) assays. We used primers located within the miR-29a/b1 and miR-29b2/c proximal promoter regions of MYC binding sites and revealed that antibodies against both MYC and HDAC3 efficiently immunoprecipitated the miR-29 promoter regions (Figures 3A and 3B). In addition, we found that site S3 of miR-29a/b1 and sites S2 and S3 of miR-29b2/c carry binding sites for both MYC and HDAC3, indicating that both MYC and HDAC3 can bind to the miR-29 promoters (Figure 3B; Figure S3A). These bindings are specific and MYC dependent, since no signal was detected at the miR-29 distal promoter (site S4) and no HDAC3 binding was detected when MYC was not bound at miR-29 promoters. These findings implicate the role of MYC in recruiting HDAC3 and suggest that HDAC3-mediated histone deacetylation might contribute to MYC-induced miR-29 gene repression. To confirm the requirement of MYC for HDAC3 binding, P493-6 cells were used to manipulate MYC expression levels. ChIP assays revealed HDAC3 binding in MYC-on and lack of binding in MYC-off P493-6 cells, supporting the recruitment role of MYC (Figure 3C). We further assessed the role of EZH2 in MYC-mediated miR-29 repression and investigated whether similar regulation patterns occur through recruitment of EZH2 and SUZ12 on miR-29a/b1 and miR-29b2/c promoters. ChIP assay with anti-EZH2 and anti-SUZ12 antibody showed that both EZH2 and SUZ12 directly bound to the miR-29 promoters in MYC-on but not in MYC-off P493-6 lymphocytes (Figure 3C) and was further validated in Burkitt and MCL cell lines (Figure 3D; Figure S3B). The loss of binding of these corepressors detected by ChIP is not due to loss of the proteins from the cell but most likely due to absence of MYC since 24 hr tet treatment resulted in loss of MYC but no change in EZH2, SUZ12, or HDAC3 expression in P493 cells (Figure 3C, insert). Of note, the EZH2 and SUZ12 binding sites correspond to the MYC and HDAC3 binding sites, supporting the role of MYC in EZH2 and SUZ12 recruitment and the role of PRC2 in silencing miR-29 expression. The variation of degree and site of MYC binding on miR-29a/b1 (site S3 only) and miR-29b2/c promoters (sites S2 and S3) likely contributes to different sensitivity of miR-29a/b1 and miR-29b2/c to the treatment of HDAC and EZH2 inhibitors. Furthermore, inhibition of PRC2 with DZNep degraded EZH2 and SUZ12 and decreased EZH2 and SUZ12 binding (Figure 3D). We next performed ChIP assay to validate the MYC, EZH2 and HDAC3 binding to miR-29 promoters in primary lymphoma samples. Four high-MYC samples of two blastic MCLs, one Burkitt and one Burkitt-like (double-hit) lymphoma, and two low-MYC indolent MCLs were chosen from our clinical samples and were used in this experiment. MYC expression levels in these samples were confirmed by fluorescence in situ hybridization (FISH) and immunohistochemical stains (data not shown). Figure 3E reveals consistent enrichment of MYC and, to a lesser extent, HDAC3 and EZH2 in miR-29 promoter regions in MYC-associated lymphomas and supports the findings that these interactions are operative in primary lymphoma cells. Taken together, these results confirm that MYC is required and a significant mediator of EZH2-mediated miR-29 repression, suggesting that HDAC3 and EZH2 have coordinated effects on miRNAs such as miR-29 expression in MYC-associated lymphomas.

To test whether MYC binding is functional, we generated luciferase reporter constructs carrying the two alternative promoters of miR-29a/b1 and miR-29b2/c at site S3 for miR29a/b1 and sites S2 and S3 for miR29b2/c and their mutated types (M2 and M3). The mutants were constructed to harbor mutations in the MYC binding site (E-box). Both wild-type and mutant plasmids (E-box mutants) were then transfected into P493-6 and 293T cells, and luciferase activity was measured (Figure 3F; Figure S3C). We found luciferase activities of wild-type miR-29a/b1 and miR-29b2/c promoters to be significantly repressed by MYC overexpression. Furthermore, knockdown of HDAC3 reversed MYC-mediated repression, supporting that HDAC3 is involved in MYC-driven miRNA repression. Compared with wild-type promoters, luciferase activity of mutated-type promoters was not significantly changed by MYC overexpression and HDAC3 knockdown. Similarly, knockdown of EZH2 reversed MYC-mediated repression in wild-type but not in mutant miR-29 promoters (Figure 3F). MYC-mediated repression was not observed in M3 of the miR-29a/b1 promoter and M2 of the miR-29b2/c promoter. This is likely attributed to the dominant function of MYC binding in site S3 of miR-29a/b1 and site S2 of miR-29b2/c promoters. These results are in line with those of ChIP experiments showing the strongest binding of MYC in S3 of miR-29a/b1 and in S2 of miR-b2/c promoters (Figure 3C). Overall, these data show that both miR-29a/b1 and miR-29b2/c loci contain MYC-binding regions that are under negative control by HDAC3 and EZH2 and that histone hypoacetylation and trimethylation contribute to MYC-induced miR-29 repression.

We further performed ChIP analysis to probe acetylated histone 4 (Ac-H4), trimethylated histone 3 (Me3-H3K27), and RNA polymerase II binding to miR-29 promoters. We first revealed that histone hypoacetylation and trimethylation are dependent on the presence of MYC since enrichment of Ac-H4 was significantly increased and Me3-H3K27 is significantly decreased in MYC-off P493-6 cells (Figure S3D). This study also revealed that accumulation of RNA polymerase II, a hallmark of active transcription, is tightly controlled by MYC. In agreement with the epigenetic silencing effect of HDAC3 and EZH2, HDAC3 knockdown and EZH2 inhibition, respectively, increased Ac-H4 and decreased Me3-H3K27 at the miR-29 promoters (Figures S3E and S3F). Of note, increased recruitment of RNA polymerase II was also observed. These results support the finding that depletion of MYC leads to reduced recruitment of HDAC3 and EZH2 and results in increased histone acetylation, decreased H3K27 trimethylation, and RNA polymerase II recruitment.

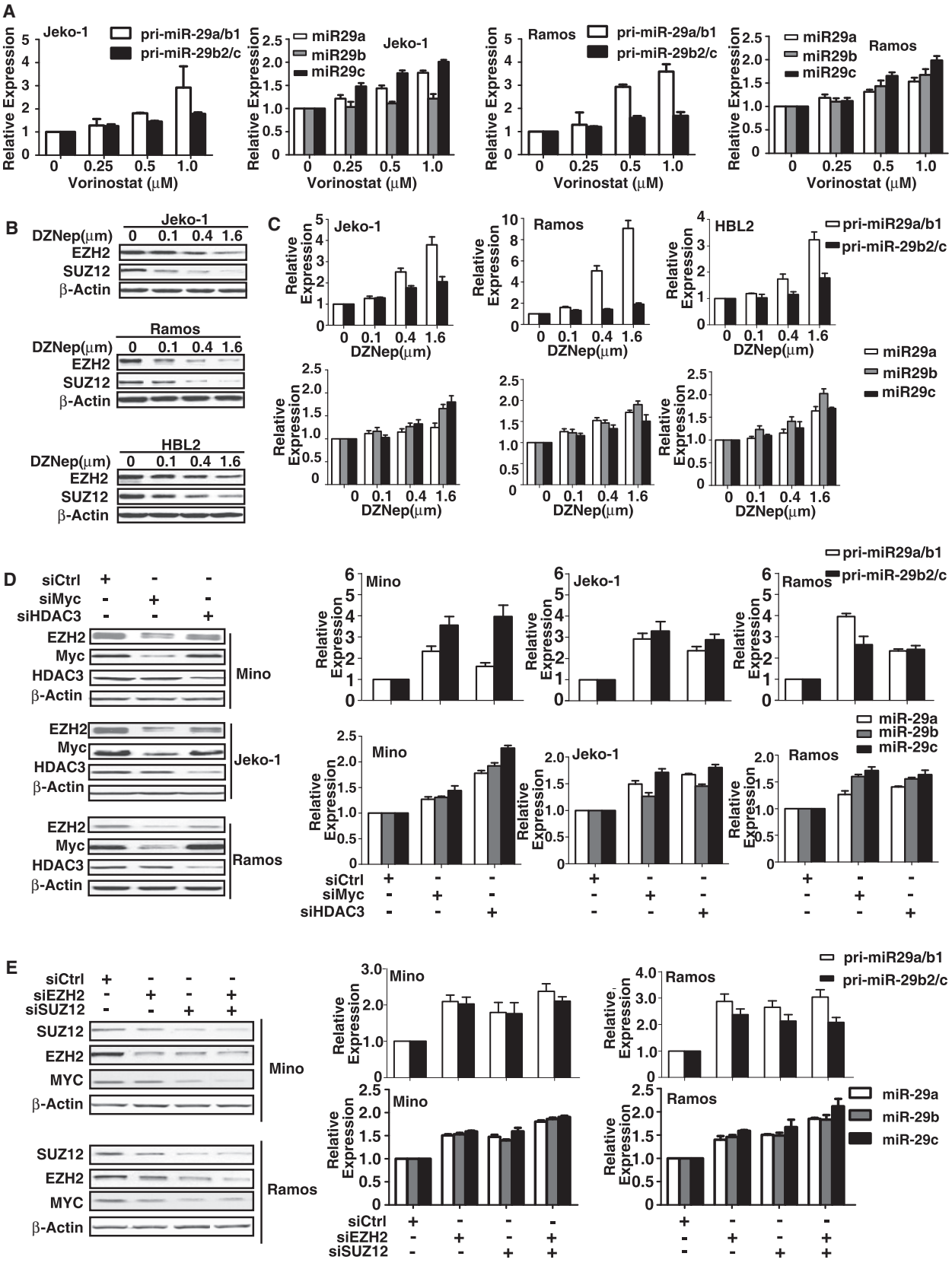
A
Jeko-1
pri-miR-29a/b1
pri-miR-29b2/c
miR29a
miR29b
miR29c
Ramos
Relative Expression
Vorinostat (μM)
B
DZNep(μm)
EZH2
SUZ12
β-Actin
C
HBL2
DZNep(μm)
D
siCtrl
siMyc
siHDAC3
Myc
HDAC3
Mino
miR-29a
miR-29b
miR-29c
E
siEZH2
siSUZ12
SUZ12
MYC

We further investigated whether PRC2 and HDAC3 form a corepressor complex with MYC to repress miR-29 expression using coimmunoprecipitation (co-IP) assays. First, 293T cells were cotransfected with vectors expressing FLAG-tagged full-length specific HDAC3 and/or with full-length MYC. When MYC and HDAC3 were cotransfected in 293T cells, the existence of MYC, HDAC3, and SUZ12, but not EZH2, was detected in the immunoprecipitates obtained with an antibody against HDAC3, and the existence of MYC and HDAC3, but not SUZ12 and EZH2, was detected in immunoprecipitates obtained with an antibody against MYC. These results indicate that MYC coimmunoprecipitated with HDAC3 and that HDAC3 coimmunoprecipitated with MYC as well as SUZ12. Next, we asked whether endogenous MYC-HDAC3-PRC2 interaction also occurred in MYC-associated lymphoma cells. Having recently demonstrated that MYC and HDAC3 formed a coimmunoprecipitate complex to regulate the miRNA expression (Zhang et al., 2012), we further examined the interaction between HDAC3 and SUZ12 in P493-6 cells. As shown in Figure 4B, cell lysates immunoprecipitated with an HDAC3-specific antibody contained HDAC3 and SUZ12. The reverse endogenous coimmunoprecipitates of HDAC3 and SUZ12 with SUZ12 antibody was also demonstrated in Jeko-1 and P493-6 cells (Figures 4B and 4C). Third, we further explored how MYC interacted with SUZ12 and EZH2 by using MYC-on and MYC-off P493-6 cells. In MYC-on P493-6 cells, strong HDAC3, weak SUZ12, and no EZH2 were coimmunoprecipitated with MYC antibody; strong SUZ12, moderate EZH2, and MYC were coimmunoprecipitated with HDAC3 antibody; strong EZH2, moderate HDAC3, and weak MYC were coimmunoprecipitated with SUZ12 antibody; and strong SUZ12, weak HDAC3, and no MYC were coimmunoprecipitated with EZH2 antibody. In contrast, in MYC-off P493-6 cells, there was no endogenous co-IP of HDAC3 and SUZ12 with MYC detected and relatively low levels of interaction of HDAC3 with SUZ12 and EZH2 (Figure 4C). Overall, these results suggest that SUZ12 and EZH2 interact with HDAC3 and MYC to form a multimolecular complex. These components interact in a linear fashion, and HDAC3 bridges the interaction between MYC and SUZ12/EZH2. To prove this, we depleted HDAC3 and tested whether this would disrupt interaction between MYC and SUZ12/EZH2 in P493-6 cells. As shown in Figure 4D, SUZ12 was not detected in MYC immunoprecipitate and MYC was not detected in SUZ12 immunoprecipitate, implicating that HDAC3 bridges the interaction between MYC and SUZ12/EZH2. These data, in conjunction with results from luciferase reporter assay, support the cooperative function of HDAC3 and EZH2 as a corepressor complex in repressing miR-29 expression.

miR-29 Is Required for MYC-Mediated Oncogenic Activity by Targeting IGF-1R and CDK6 Pathways in MCL and Other MYC-Expressing B-Cell Lymphomas

We investigated whether downregulation of miR-29 is necessary for cellular transformation induced by oncogenic MYC overexpression. In addition to *CDK6*, our bioinformatic analysis also revealed *IGF-1R* as a potential target of miR-29. Increased expression of miR-29 significantly downregulated IGR-1R (Figure 5A; Figure S4A). The relative luciferase activity of the wild-type construct of *IGF-1R* 3′-UTR was reduced by overexpression of miR-29c and was increased when miR-29c was knocked down, whereas such effects of miR-29c on luciferase activity were not observed with the mutant construct of *IGF-1R* 3′-UTR (Figure 5A). These findings support a direct and specific interaction of miR-29c on *IGF-1R* 3′-UTR. To confirm the relevance of the expression of IGF-1R and the relationship between miR-29 and IGF-1R, the expression of miR-29 and IGF-1R expression were assessed in a set of primary MCL tissues and normal B lymphocytes. An inverse correlation of miR-29 and IGF-1R protein expression was observed in all MCL samples by using Pearson coefficient, and correlation coefficients were calculated identifying IGF-1R as a miR-29 target in addition to the previously demonstrated CDK6 in MCL (Zhao et al., 2010; Figure 5B; Figures S4B and S4C).

Given the oncogenic feature of MYC and regulatory role of MYC in miR-29 expression, we postulated that MYC-mediated miR-29 repression and subsequent miR-29 target changes contribute to MYC-driven lymphoma cell growth and proliferation. We, therefore, tested whether MYC upregulates miR-29 targets (CDK6 and IGF-1R expression) in MYC-on and MYC-off P493-6 cells. With MYC turn-on, protein levels of CDK6 and IGF-1R were significantly increased, whereas they were significantly downregulated with MYC turn-off (Figure 5C). In contrast, mRNA levels of *CDK6* and *IGF-1R* were not significantly influenced by MYC (Figure S4D). These data suggest a posttranscriptional mechanism of CDK6 and IGF-1R expression and are in line with MYC-driven miR-29-mediated regulation of CDK6 and IGF-1R expression. Of note, when MYC is turned off (MYC-off cells), IGF-1R declines at a faster rate than CDK6. This may be related to differences in the mRNA and/or protein half-life of these two proteins. We further assessed whether miR-29 mediated MYC-driven CDK6 and IGF-1R induction and cell growth in MYC-expressing lymphoma cells. In P493-6 cells, the ectopic forced expression of miR-29 abolished MYC-induced CDK6 and IGF-1R expression, and miR-29 knockdown blocked MYC-off-mediated CDK6 and IGF-1R repression (Figure 5D; Figure S4A). Furthermore, knockdown of CDK6 and IGF-1R induced significant inhibition of cell growth and colony formation, and the combined inhibition of CDK6 and IGF-1R resulted

Figure 2. MiR-29 Family Is Coregulated by HDAC3 and PRC2

(A) Vorinostat treatment for 48 hr dose-dependently increased primary and mature miR-29 expression levels in Jeko-1 and Ramos cells.

(B) DZNep treatment for 48 hr downregulated EZH2 and SUZ12 in Jeko-1, Ramos, and HBL2 cells.

(C) DZNep treatment for 48 hr dose-dependently increased primary and mature miR-29 expression in Jeko-1, Ramos, and HBL2 cells.

(D) Knockdown of MYC or HDAC3 by siRNAs increased pri-miR-29 and mature miR-29 expression levels in Mino, Jeko-1, and Ramos cells. mRNA and miRNA expression levels of cells treated with siCtrl were arbitrarily set as 1.

(E) Knockdown of EZH2 and SUZ12 by their siRNAs increased miR-29a-c gene expression in Mino and Ramos cells. Results in (A) through (E) are means ± SD from at least 3 biological replicates.

See also Figure S2.

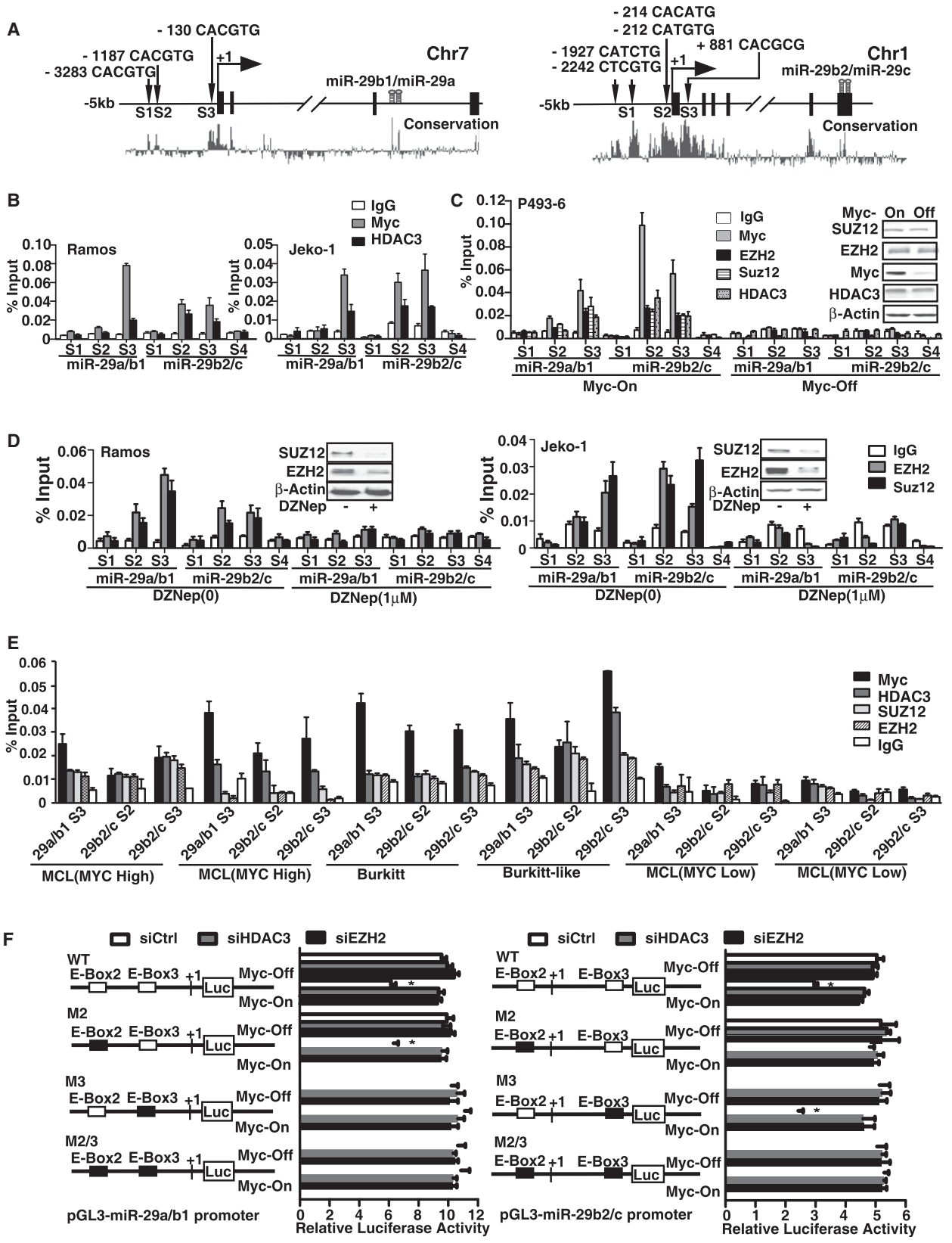
A
- 130 CACGTG
- 1187 CACGTG
- 3283 CACGTG
+1
Chr7
miR-29b1/miR-29a
-5kb
S1S2
S3
Conservation
- 214 CACATG
- 212 CATGTG
- 1927 CATCTG
- 2242 CTCGTG
+ 881 CACGCG
Chr1
miR-29b2/miR-29c
S1
S2
S3
B
Ramos
Jeko-1
IgG
Myc
HDAC3
% Input
miR-29a/b1
miR-29b2/c
C
P493-6
IgG
Myc
EZH2
Suz12
HDAC3
Myc- On Off
SUZ12
EZH2
Myc
HDAC3
β-Actin
Myc-On
Myc-Off
D
Ramos
Jeko-1
SUZ12
EZH2
β-Actin
DZNep - +
IgG
EZH2
Suz12
DZNep(0)
DZNep(1μM)
E
Myc
HDAC3
SUZ12
EZH2
IgG
29a/b1 S3
29b2/c S2
29b2/c S3
MCL(MYC High)
MCL(MYC High)
Burkitt
Burkitt-like
MCL(MYC Low)
MCL(MYC Low)
F
siCtrl
siHDAC3
siEZH2
WT
M2
M3
M2/3
E-Box2
E-Box3
+1
Luc
Myc-Off
Myc-On
pGL3-miR-29a/b1 promoter
pGL3-miR-29b2/c promoter
Relative Luciferase Activity

in a more marked inhibition of cell growth and colony formation (Figure 5E; Figure S4E). Accordingly, miR-29 overexpression as well as MYC knockdown significantly abrogated lymphoma colony formation capacity (Figure 5F; Figures S4F and S4G).

MYC-miR-26a-EZH2-miR-494 Positive Feedback Loop Sustains MYC Activity and miR-29 Repression in MCL and Other Aggressive B-Cell Lymphomas

Accumulating evidence has indicated MYC-dependent regulation of EZH2, with further evidence revealing the ability of EZH2 to induce MYC expression (Sander et al., 2008; Lu et al., 2011). We speculated that a feedback loop existed between MYC and EZH2, thereby maintaining MYC overexpression and miR-29 repression in MYC-associated lymphomas. We thus explored the interaction between MYC and EZH2 and examined the role of this circuitry in sustaining miR-29 repression. First, we tested whether MYC stimulates EZH2 expression by repression of its negative regulator miRNAs. Since EZH2 was identified by TargetScan as a potential miR-26a target and was recently experimentally validated (Sander et al., 2008), we examined the effects of miR-26a on EZH2 expression. Overexpression of miR-26a reduced EZH2 and MYC protein abundance in Jeko-1 and Mino cells, and ectopic expression of miR-26a inhibited *EZH2* 3′-UTR luciferase reporter activity (Figure 6A), confirming that miR-26a regulates EZH2. Given that miR-26a is a reported MYC-regulated miRNA, we next used the P493-6 cells to confirm and explore the mechanism by which MYC induces EZH2 expression. Expression of miR-26a in MYC-on P493-6 cells was significantly lower than that shown in MYC-off cells (Figure 6B). Furthermore, the effects of MYC on EZH2 expression were examined, revealing that mRNA levels of *EZH2* and *SUZ12* were not changed, whereas protein levels were significantly increased in MYC-on cells and decreased in MYC-off cells (Figure 6B; Figure S5A). This result implies that MYC regulated EZH2 via posttranscriptional regulation. Moreover, ectopic expression of miR-26a blocked MYC-induced EZH2 expression in MYC-on P493-6 cells. To substantiate that miR-26a expression is responsible for MYC-induced EZH2 change, we inhibited miR-26a by using anti-miR-26a and revealed increased EZH2 expression in MYC-off P493-6 cell (Figure 6C), further supporting the role of miR-26a in MYC-regulated EZH2 expression. We next tested whether EZH2 stimulates MYC expression. Figure 6D shows that inhibition of EZH2 by using DZNep and shRNA against EZH2 significantly decreased MYC expression, substantiating the regulatory role of EZH2 in MYC expression and implying a positive feedback loop of MYC and EZH2. We reasoned that EZH2 induces MYC expression through repression of MYC-repressing miRNAs. Thus, we next explored the EZH2-regulated miRNAs by examining the effects of EZH2 inhibition on the expression of miRNAs. miRNA microarray was performed and the expression profile from Jeko-1 cells after 72 hr DZNep (2 μM) treatment was determined (Figure S5B). We identified a set of miRNAs that were upregulated by DZNep, were downregulated by PRC2, and are predicted to target MYC (Figures 6E and 6F). To further test whether these miRNAs target the *MYC* 3′-UTR directly, we cloned the full length of *MYC* 3′-UTR and constructed a luciferase reporter plasmid (p-miR-*MYC*-3′-UTR-WT). The plasmid was cotransfected into 293T cells, with each of the aforementioned pre-miRNAs and luciferase activity measured. Figure S5C shows that the luciferase activity of wild-type *MYC* reporter were reduced by overexpression of miR-135, miR-200, and miR-374, as well as most noticeably decreased by miR-494 overexpression. With TargetScan predicting that *MYC* 3′-UTR contains two miR-494-binding sites, we subsequently mutated the miR-494 binding sites in *MYC* 3′-UTR to test whether miR-494 specifically targets *MYC* 3′-UTR. As revealed in Figure 6F, the mutation abolished the suppressive effect of miR-494 on the luciferase reporter activity. These results demonstrated that the miR-494 specifically and directly targeted the *MYC* gene. To determine whether miR-494 is required and a significant mediator for EZH2-mediated MYC induction, we performed qRT-PCR and validated that miR-494 was upregulated by EZH2 inhibition through DZNep treatment and shEZH2 or siEZH2 (Figures S5D and S5E). To further confirm that miR-494 is directly regulated by EZH2, ChIP assay was performed and showed the direct EZH2 binding to miR-494 promoter regions. Furthermore, this binding is inhibited by the depletion of EZH2 through DZNep treatment (Figure S5F). We next showed that overexpression of miR-494 downregulated MYC protein level (Figure 6G). Accordingly,

Figure 3. MYC Recruits HDAC3 and PRC2 to miR-29 Promoters to Repress the miR-29 Transcription through Histone Deacetylation and Trimethylation

(A) Schematic diagram showing location of MYC-binding sites of pri-miR-29a/b1 and pri-miR-29b2/c regulatory region. Sites S1, S2, and S3 represent MYC-binding site, which has an E-box sequence. S4 was used as negative control and is located in the intron 4 of pri-miR-29b2/c and without E-box in this region. Both pri-miR-29s are highly conserved in their putative promoter region and in the pre-miR-29 stem sequences, encoded in the last intron (pre-miR-29a/b1) on chr.7q32.3 and the last exon (pre-miR-29b2/c) on chr.1q32.2, respectively.

(B) ChIP assay showing MYC and HDAC3 enrichment on pri-miR-29a/b1 and pri-miR-29b2/c promoters. ChIP assay was performed using MYC or HDAC3 antibody to detect binding on S1–S3 regions of pri-miR-29a/b1 and pri-miR-29b2/c promoters, and S4 was used as a negative control. Percent input was calculated with $2^{(Ct\ [1\%\ of\ input] - Ct\ [ChIP])}$. Ct, cycle threshold.

(C) ChIP assay showing MYC, HDAC3, EZH2, and SUZ12 enrichment on pri-miR-29a/b1 and pri-miR-29b2/c promoters and dependence of HDAC3 and EZH2/SUZ12 binding on MYC in P493-6 cells with or without 24 hr tet treatment, Inserts, western blots showing protein level of MYC, HDAC3, and EZH2/SUZ12 in MYC-on and MYC-off (24 hr tet treatment) P493-6 cells.

(D) ChIP assay showing EZH2 and SUZ12 enrichment on pri-miR-29a/b1 and pri-miR-29b2/c with or without DZNep treatment.

(E) ChIP assay showing MYC, HDAC3, EZH2, and SUZ12 enrichment on pri-miR-29a/b1 and pri-miR-29b2/c promoters in primary lymphoma samples with high MYC expression (blastic MCLs, Burkitt, or Burkitt-like lymphomas) and no enrichment in primary samples with low MYC expression (indolent MCLs).

(F) Schematic diagram of pri-miR-29a/b1 and pri-miR-29b2/c promoter luciferase reporter. Solid boxes represent point mutation of E-Box. P493-6 cells were transfected with either wild-type or mutants (M) of pri-miR-29a/b1 or pri-miR-29b2/c promoter luciferase reporter, together with siHDAC3, siEZH2, or nontargeting siRNA. The luciferase activity is normalized to β-galactosidase. Results are means ± SD from three biological replicates. For ChIP assays, IgG was used as a negative control. In (B) through (F), results are means ± SD from at least three biological replicates. Insets, western blots showing protein level.

See also Figure S3.

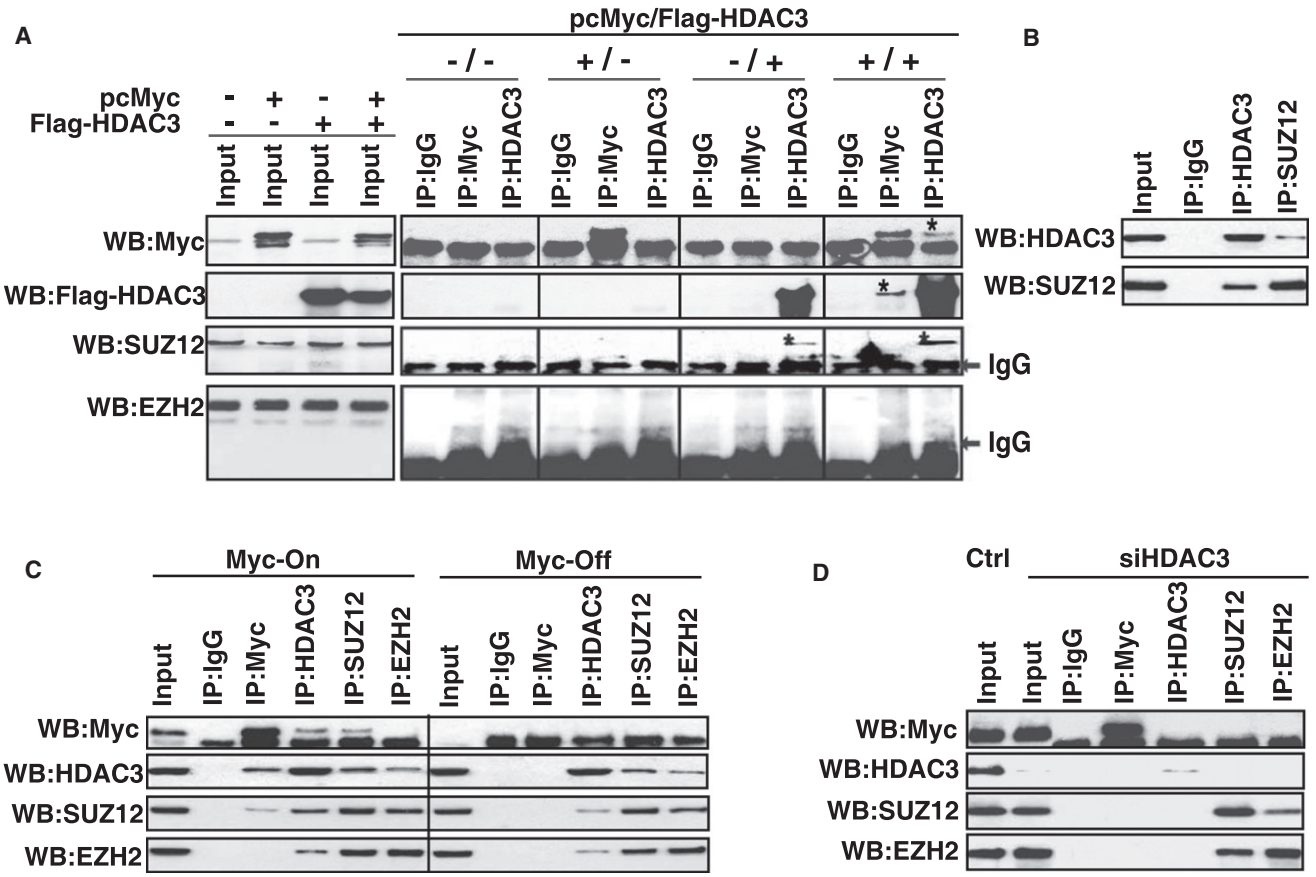

Figure 4. HDAC3 Bridges the Interaction between MYC and PRC2 to Form a Corepressor Complex

(A) 293T cells were transfected with MYC plasmid or FLAG-HDAC3 plasmid or cotransfected with MYC plasmid and FLAG-HDAC3 plasmid. The whole cell lysates were immunoprecipitated using an antibody against MYC, HDAC3, and control IgG, followed by western blot with an antibody against MYC, FLAG, SUZ12, and EZH2.

(B) Reciprocal co-IP showing endogenous co-IP of HDAC3 and SUZ12. Whole cell extracts of Jeko-1 cells were subjected to IP with anti-HDAC3 antibody followed by western blotting for SUZ12, and similar whole cells extracts were subjected to IP with anti-SUZ12, followed by western blotting with anti-HDAC3.

(C) Co-IP of MYC, HDAC3, and SUZ12/EZH2 in MYC-on and MYC-off P493-6 cells. Cell lysates of P493-6 with and without tet treatment were immunoprecipitated with MYC, HDAC3, SUZ12, EZH2, and control IgG, respectively, followed by western blotting with an antibody against MYC, HDAC3, SUZ12, and EZH2.

(D) HDAC3-mediated interaction between MYC and SUZ12/EZH2. P493-6 (MYC-on) cells were transfected with HDAC3 siRNA or nontargeting siRNA to knock down HDAC3, and co-IP experiments were performed to evaluate interaction between MYC and SUZ12/EZH2. In (A) through (D), input is equivalent to 10% of the lysate used for the co-IP. Results are representative of three independent experiments.

downregulation of EZH2 was also observed, supporting the presence of a MYC-miR-26a-EZH2-miR-494 feed-forward circuit sustaining MYC activity and miR-29 repression.

To address whether the above observations in MCL and Ramos cell lines are relevant to other aggressive cell lines and primary lymphoma cells, we examined the relationship between MYC, EZH2, and miR-26a as well as miR-29 expression levels in MYC-expressing lymphoma cell lines and primary MYC-expressing lymphomas. The cell lines included two transformed large B lymphoma cell lines (SUDHL4, SUDHL10); the Epstein-Barr virus (EBV)-associated lymphoma cell line SKW6.4; aggressive MCL cell lines Jeko-1, Mino-1, HBL-2, NCEB-1, Rec-1, and Z138c; and Burkitt lymphoma cell lines Raji and Ramos. The primary lymphomas included Burkitt lymphomas, high-grade transformed diffuse large cell lymphomas, and MCLs. For comparison, we also included normal control B lymphocytes as control, with MYC-on and MYC-off P493-6 cells as positive and negative cell lines. In line with our hypothesis, low expression levels of miR-29 family and miR-26a were correlated with high expression of MYC and EZH2, and correlation coefficients were calculated in these cell lines and primary samples by using Pearson coefficient (Figures 7A–7D). When compared with normal control B lymphocytes, MYC expression was positively correlated with EZH2 expression in these primary samples. Collectively, these observations provide EZH2 and HDAC3 as potential therapeutic targets for aggressive B-cell lymphomas.

Combined Inhibitors of HDAC and EZH2 Cooperatively Derepressed miR-29 and Suppressed Tumor Growth In Vitro and In Vivo in MCL and Other Aggressive B-Cell Lymphomas

In light of the importance of low or absent expression of miR-29 in MCL aggressive progression and the ability of miR-29 expression to inhibit tumor cell growth, reactivation of miR-29

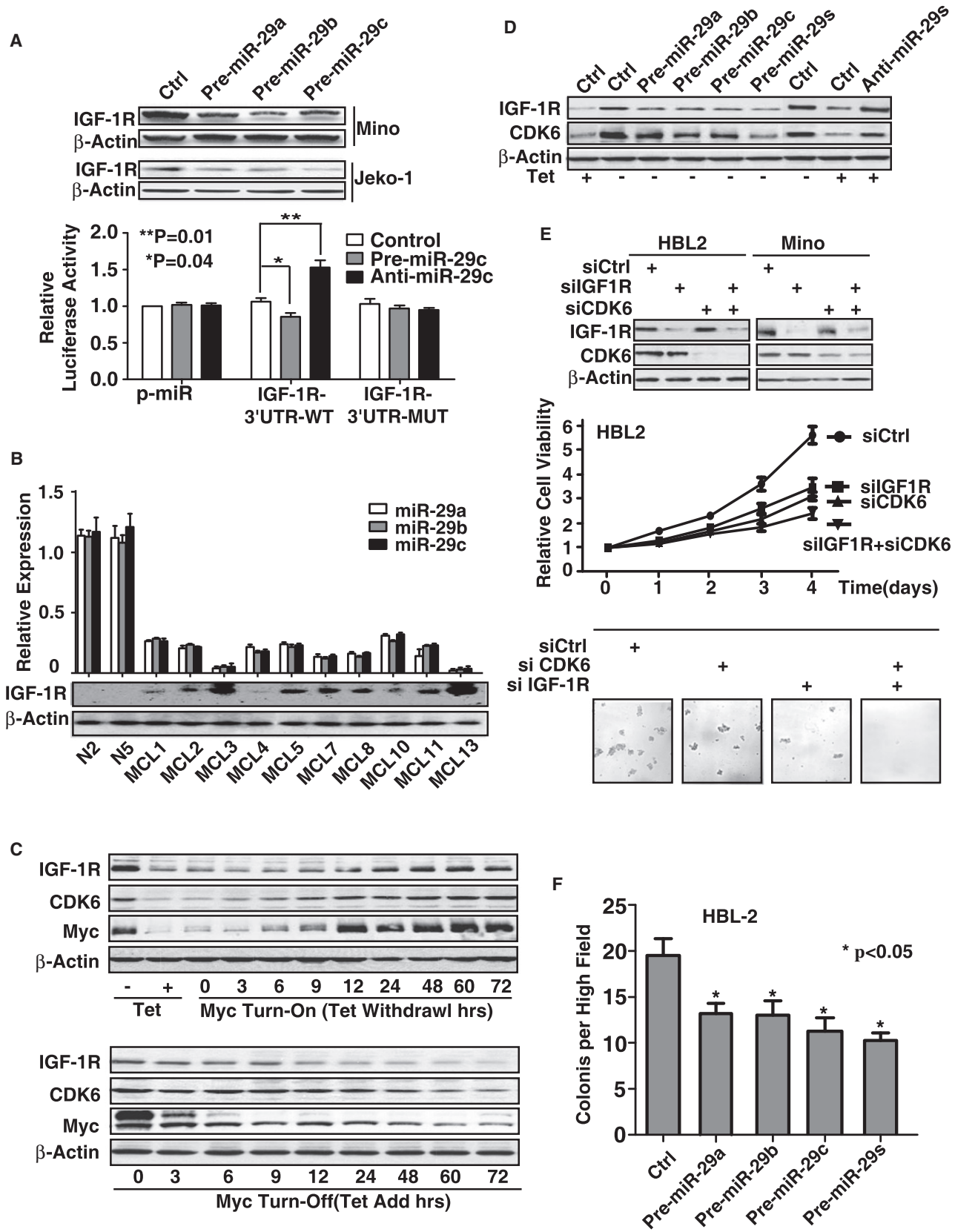
A
Ctrl
Pre-miR-29a
Pre-miR-29b
Pre-miR-29c
IGF-1R
β-Actin
Mino
Jeko-1
Relative Luciferase Activity
**P=0.01
*P=0.04
Control
Pre-miR-29c
Anti-miR-29c
p-miR
IGF-1R-3'UTR-WT
IGF-1R-3'UTR-MUT
B
Relative Expression
miR-29a
miR-29b
miR-29c
N2
N5
MCL1
MCL2
MCL3
MCL4
MCL5
MCL7
MCL8
MCL10
MCL11
MCL13
C
CDK6
Myc
Tet
Myc Turn-On (Tet Withdrawl hrs)
Myc Turn-Off(Tet Add hrs)
D
Ctrl
Pre-miR-29a
Pre-miR-29b
Pre-miR-29c
Pre-miR-29s
Anti-miR-29s
Tet
E
HBL2
Mino
siCtrl
siIGF1R
siCDK6
Relative Cell Viability
siIGF1R+siCDK6
Time(days)
si CDK6
si IGF-1R
F
HBL-2
* p<0.05
Colonis per High Field

represents a promising therapeutic approach for this tumor type. Given that HDAC3 and EZH2 converged at miR-29 promoters to repress miR-29 expression and suppression of CDK6 and IGF-1R pathways by miR-29, we next tested whether inhibition of HDAC and EZH2 cooperatively restored miR-29 expression and subsequently inhibited CDK6 and IGF-1R to block the clonenogenic growth in soft agar and lymphoma growth in vivo. We also asked whether combined inhibitors of HDAC and PRC2 are more effective in induction of miR-29 expression, suppression of CDK6 and IGF-1R, and tumorigenicity in vivo. Compared with each agent alone, cotreatment with vorinostat and DZNep induced significantly higher expression of pri-miR-29a/b1, pri-miR-29b2/c, and mature miR-29 than each agent alone in HBL2, Ramos, and Mino, as well as Z138c MCL cells (Figure 8A; Figures S6A–S6D). Both DZNep and vorinostat resulted in enhanced inhibition of colony formation with corresponding downregulation of CDK6 and IGF-1R in HBL2 and Z138c cells (Figures 8B and 8C; Figure S6B). Next, we compared the effects of DZNep and/or vorinostat on the viability of transformed and nontransformed lymphocytes by using P493-6 cells. Figure 8D demonstrates that exposure to DZNep or vorinostat induced more loss of viability in MYC-on than in MYC-off P493-6 cells. Finally, we determined whether the combination of DZNep and vorinostat would also exert increased in vivo antilymphoma activity. Figures 8E and 8F show that cotreatment with DZNep and vorinostat inhibits tumor growth and significantly improves survival of nonobese diabetic/severe combined immunodeficient (NOD/SCID) mice bearing lymphoma xenografts. Lymphoma size was remarkably reduced and survival of NOD/SCID mice with lymphoma was significantly higher when they were treated with DZNep plus vorinostat than when treated with vorinostat, DZNep, or vehicle alone. Furthermore, to confirm that the in vivo targets of these inhibitors were inhibited, western blot was performed and revealed that vorinostat and/or DZNep treatment resulted in significant downregulation of EZH2, SUZ12 and downstream target IGF-1R, as well as MYC from harvested lymphoma tissues (Figure S6E). In addition, to validate the direct role of corepressors EZH2 and HDAC3 in lymphoma formation in vivo, two independent genetic approaches were used. HBL2 cells were first transfected with siRNAs or shRNAs against EZH2 or HDAC3 to deplete their expression, and, subsequently, these cells were applied to an in vivo lymphoma formation experiment as described in Figure 8E. Figures S6F and S6G confirmed that HDAC3 or EZH2 siRNA or shRNA knocked down EZH2 or HDAC3, respectively, and significantly abolished lymphoma growth in vivo supporting the role of EZH2 and HDAC3 in lymphoma formation. To support that the tumor inhibition is due to decreased proliferation, the proliferation status of the tumor cells in shEZH2- and shHDAC3-treated HBL2 xenografts was measured by using proliferation marker genes *Ki-67* and *PCNA*. Figure S6H shows that the *Ki-67* and *PCNA* genes were indeed significantly decreased in shEZH2 and shHDAC3 groups when compared to shCtrl group, indicating that the tumor suppression by shEZH2/HDAC3 is at least partially through proliferation inhibition. Taken together, MYC-mediated miR-29 repression through coordinated epigenetic silencing of HDAC3 and EZH2 is a important therapeutic target of histone modifications in aggressive B-cell lymphomas.

DISCUSSION

This study was undertaken to investigate (1) the potential interplay between MYC and histone modifiers HDAC3 and EZH2 and their role in miR-29 gene repression, (2) the role of the miR-29 family and their downstream targets in MYC-driven oncogenesis, (3) the underlying mechanism of persistent MYC activation in these aggressive lymphomas through a MYC-miRNA-EZH2 positive feedback loop, and (4) whether HDAC3 and EZH2 cooperatively regulate miR-29 expression and, accordingly, whether inhibitors of HDAC and EZH2 restore expression of miR-29 in MYC-transformed B lymphoma cells to significantly inhibit tumorigenesis ex vivo and in vivo. Our findings indicate that miR-29 repression is a result of MYC/HDAC3 and EZH2 interaction and contributes to aggressive clinical outcome of MYC-associated lymphomas. Results of this study led to the identification of a model for interplay between MYC, HDAC3, PRC2, and miRNAs and their contribution to MYC-associated lymphomagenesis and HDAC3/EZH2/miR-29 as significant therapeutic targets for aggressive lymphomas. We showed that MYC, HDAC3, and PRC2 form a repressive complex tethered to miR-29 promoter elements to epigenetically repress miR-29 transcription in MYC-expressing lymphoma cells. Subsequent miR-29 downregulation resulted in induction of CDK6 and IGF-1R and mediated MYC-driven lymphomagenesis shown in Figure 8G. Furthermore, we demonstrated that MYC contributed to the upregulation of EZH2 via repressing EZH2-targeting miR-26a and that EZH2, in turn, induced MYC expression via MYC-targeting miR-494, thereby generating a positive feedback loop to ensure persistent high protein levels of MYC and EZH2 and further repression of miR-29, which could be involved in maintaining the malignant phenotype. In addition

Figure 5. miR-29 Is Required for MYC-Mediated Oncogenic Activity by Targeting IGF-1R and CDK6 Pathways

(A) IGF-1R is a direct target of miR-29. Overexpression of miR-29a-c downregulates IGF-1R expression and reduces luciferase activity of wild-type *IGF-1R*-3′ UTR reporter (*IGF-1R*-WT) but not mutated *IGF-1R*-3′UTR reporter (*IGF-1R*-M).

(B) miR-29 level is reversely correlated with IGF-1R protein expression of MCL patient samples.

(C) IGF-1R and CDK6 expression in MYC-on and MYC-off P493-6 cells.

(D) Overexpression of miR-29 after 48 hr pre-miR-29a-c transfection abolished MYC-induced CDK6 and IGF-1R expression and knockdown of miR-29 by anti-miR-29s (pool of anti-miR-29a-c) transfection blocked MYC-off-induced CDK6 and IGF-1R repression.

(E) Knockdown of IGF1R and CDK6 by their siRNAs inhibits lymphoma cell survival measured by MTT assay and colony formation assay in HBL2 cells after transfection with siIGF-1R and siCDK6 or control siRNA. Micrographs show the appearance of colonies in methycellulose gels at low power.

(F) Overexpression of miR-29 decreases the colony formation. The numbers of tumor colonies were enumerated microscopically after an incubation of 2 weeks. Results are representative of three independent experiments or means ± SD from at least three biological replicates.

See also Figure S4.

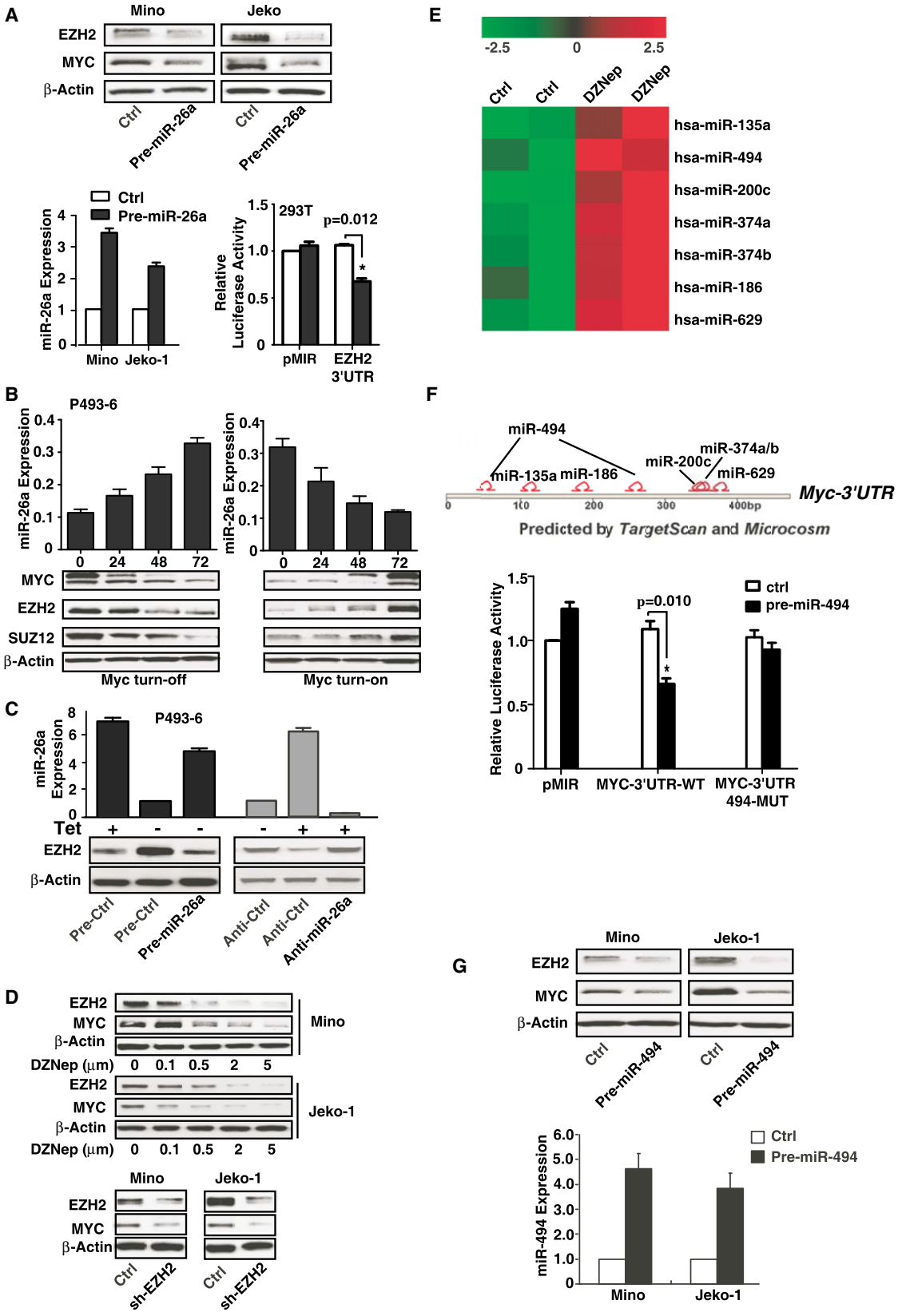
A
Mino
Jeko
EZH2
MYC
β-Actin
Ctrl
Pre-miR-26a
Ctrl
Pre-miR-26a
Ctrl
Pre-miR-26a
miR-26a Expression
Mino
Jeko-1
293T
p=0.012
Relative Luciferase Activity
pMIR
EZH2 3'UTR
B
P493-6
miR-26a Expression
0
24
48
72
MYC
EZH2
SUZ12
β-Actin
Myc turn-off
Myc turn-on
C
P493-6
miR-26a Expression
Tet
EZH2
β-Actin
Pre-Ctrl
Pre-Ctrl
Pre-miR-26a
Anti-Ctrl
Anti-Ctrl
Anti-miR-26a
D
EZH2
MYC
β-Actin
Mino
DZNep (μm) 0 0.1 0.5 2 5
Jeko-1
Mino
Jeko-1
Ctrl
sh-EZH2
Ctrl
sh-EZH2
E
-2.5
0
2.5
Ctrl
Ctrl
DZNep
DZNep
hsa-miR-135a
hsa-miR-494
hsa-miR-200c
hsa-miR-374a
hsa-miR-374b
hsa-miR-186
hsa-miR-629
F
miR-494
miR-374a/b
miR-135a
miR-186
miR-200c
miR-629
Myc-3'UTR
Predicted by TargetScan and Microcosm
Relative Luciferase Activity
p=0.010
ctrl
pre-miR-494
pMIR
MYC-3'UTR-WT
MYC-3'UTR 494-MUT
G
Mino
Jeko-1
EZH2
MYC
β-Actin
Ctrl
Pre-miR-494
Ctrl
Pre-miR-494
miR-494 Expression
Ctrl
Pre-miR-494
Mino
Jeko-1

to miR-494 other miRNAs such as miR-135a, miR-186, and miR-200c are also regulated by EZH2 and, in turn, may cooperatively regulate MYC expression. Treatment with pan-HDAC inhibitor vorinostat, EZH2 inhibitor DZNep, and their specific siRNAs disrupt the MYC-miRNA-EZH2 regulatory circuitry, resulting in enhanced restoration of miR-29 expression, downregulation of miR-29 target genes *CDK6* and *IGF-1R*, and suppression of lymphoma cell growth (Figures S6D and S6F). Moreover, several other tumor suppressors and oncogenes such as *TCL-1* and *MCL1* (Pekarsky et al., 2006; Mott et al., 2007) are also regulated by miR-29 and may contribute to miR-29-mediated oncogenesis. On the other hand, a recent study implicated that miR-29 can function as an oncogene in indolent chronic lymphocytic leukemia (CLL), suggesting that miR-29 can function as either a tumor suppressor or an oncogene depending on the cellular context (Pekarsky et al., 2006). Our findings indicated that miR-29 is a tumor suppressor in aggressive MCL and revealed critical mechanisms for MYC-driven miRNA suppression and rational therapeutic targets of histone modifications in aggressive B-cell malignancies. These data also indicate that MYC-driven miR-29 repression through recruitment of HDAC3 and/or EZH2 could be a generic mechanism for miRNA silencing in aggressive B-cell lymphomas. The MYC-driven miRNA repression may underlie the molecular mechanism for lymphoma aggressive transformation and can be epigenetically targeted through manipulation of histone modifications.

We identified a regulatory element (site S3) located ~5 kb upstream from the miR-29a/b1 and two regulatory elements (sites S2 and S3) located ~5 kb upstream from tthe miR-29b2/c cluster. These elements contain a MYC-binding site (or sites) that also associate with the transcriptional repressor factors EZH2 and HDAC3. Co-IP assays revealed that MYC coimmunoprecipitates with HDAC3 and HDAC3 with EZH2, likely through SUZ12 to form a MYC-HDAC3-PRC2 complex. These findings support the notion that MYC repressed miR-29a/b1 and miR-29b2/c through recruitment and interaction with HDAC3 and PRC2 as a corepressor complex. Given that miR-29a/b1 and miR-29b2/c are located in the different chromosomes, have different promoter regions and MYC-binding sites, miR-29 transcripts indeed respond differently to the presence or absence of MYC, EZH2, and HDAC3 as shown in Figures 1 and 2. Furthermore, ChIP analysis demonstrated that MYC, HDAC3, and PRC2 colocalize to the promoters of the miR-29 cluster genes and that HDAC3 and EZH2/PRC2 binding to miR-29 promoters was MYC dependent, supporting the role of MYC in the recruitment of HDAC3 and PRC2 to the miR-29 promoters. Finally, luciferase reporter assays demonstrated that miR-29 is repressed by MYC acting through HDAC3 and EZH2-mediated histone deacetylation and trimethylation. Recent work has shown that MYC is involved in miR-29 gene expression regulation and that HDAC with MYC is responsible for the silencing of miR-29b in acute myeloid leukemia cells (Liu et al., 2010). Our current findings suggest that PRC2 is an additional factor ensuring miR-29 downregulation through working in concert with HDAC3. Thus, these findings define a key mechanism of miRNA transcriptional repression by MYC and shed light on the poorly understood mechanisms involved in miRNA suppression in B-cell lymphomas.

The MYC-miR-26a-EZH2-miR-494 positive feedback loop was observed in MYC-expressing lymphoma cell lines and primary lymphoma cells examined. We conclude that miR-26a can function as a tumor suppressor miRNA in MYC-associated lymphomas. Once MYC is activated, miR-26a is repressed; the more miR-26a is decreased, the more its target gene (such as *EZH2*) is activated. Inverse correlations between miR-26a, miR-29, and MYC, EZH2 expression were detected in both cell lines and primary samples supporting the presence of MYC-miRNA-EZH2 positive feedback loop. The decrease in miR-26a expression and consequent increase in EZH2 expression have been reported in a variety of aggressive tumors such as hepatocellular carcinoma, nasopharyngeal carcinoma, and Burkitt lymphoma (Sander et al., 2008). The frequent EZH2 overexpression found in human cancers is associated with more aggressive cancer phenotypes with poor prognosis (So et al., 2011). This was further supported by findings in a larger cohort of hepatocellular carcinoma patients, where low miR-26a expression was associated with shorter overall survival (Kota et al., 2009). In addition, EZH2 was detected in the neoplastic large cells in intermediate- and high-grade B-cell lymphomas, and its expression was correlated with clinical grade and the presence of Ki-67 expression (van Kemenade et al., 2001). In MCL, EZH2 is upregulated in proliferating MCL cells, with expression levels of MYC and EZH2 being the strongest prognostic factors independent of tumor proliferation and clinical factors of MCL (Visser et al., 2001). These reports concur with our previous and current findings that miR-29 expression is reversely correlated, controlled with MYC and EZH2, and associated with MCL aggressive progression (Zhao et al., 2010). Our significant finding of the MYC-EZH2-miR-29 axis provides insight into how EZH2 is activated and contributes to tumor aggressive transformation,

Figure 6. MYC-miR-26a-EZH2-miR-494 Positive Feedback Loop Sustains MYC Activity and miR-29 Repression

(A) EZH2 is a direct target of miR-26a. Overexpression of miR-26a downregulates EZH2 and MYC expression and suppresses EZH2 3′-UTR luciferase activity in 293T cells.

(B) miR-26a expression is regulated by MYC. miR-26a, EZH2, SUZ12, and MYC protein expression levels in MYC turn-on and MYC turn-off P493-6 cells.

(C) Overexpression of miR-26a by pri-miR-26a suppresses MYC-induced EZH2 expression in MYC-on P493-6 cells, while suppression of miR-26a by anti-miR-26a increases EZH2 expression in MYC-off P493-6 cells.

(D) Inhibition of EZH2 with DZNep or shRNA decreases MYC protein expression.

(E) Putative *MYC* 3′-UTR targeting miRNAs are upregulated by EZH2 inhibition.

(F) TargetScan and microCosm depicting potential binding sites for the DZNep upregulated miRNAs in *MYC*-3′-UTR and MYC is a direct target of miR-494. 293T cells are cotransfected with luciferase reporters, which contain the wild-type or mutant of *MYC* 3′-UTR, and overexpression of miR-494 inhibits *MYC*-3′-UTR but not mutant 3′-UTR luciferase activities.

(G) Overexpression of miR-494 suppresses MYC and EZH2 expression. Results are representative of three independent experiments or means ± SD from at least three biological replicates.

See also Figure S5.

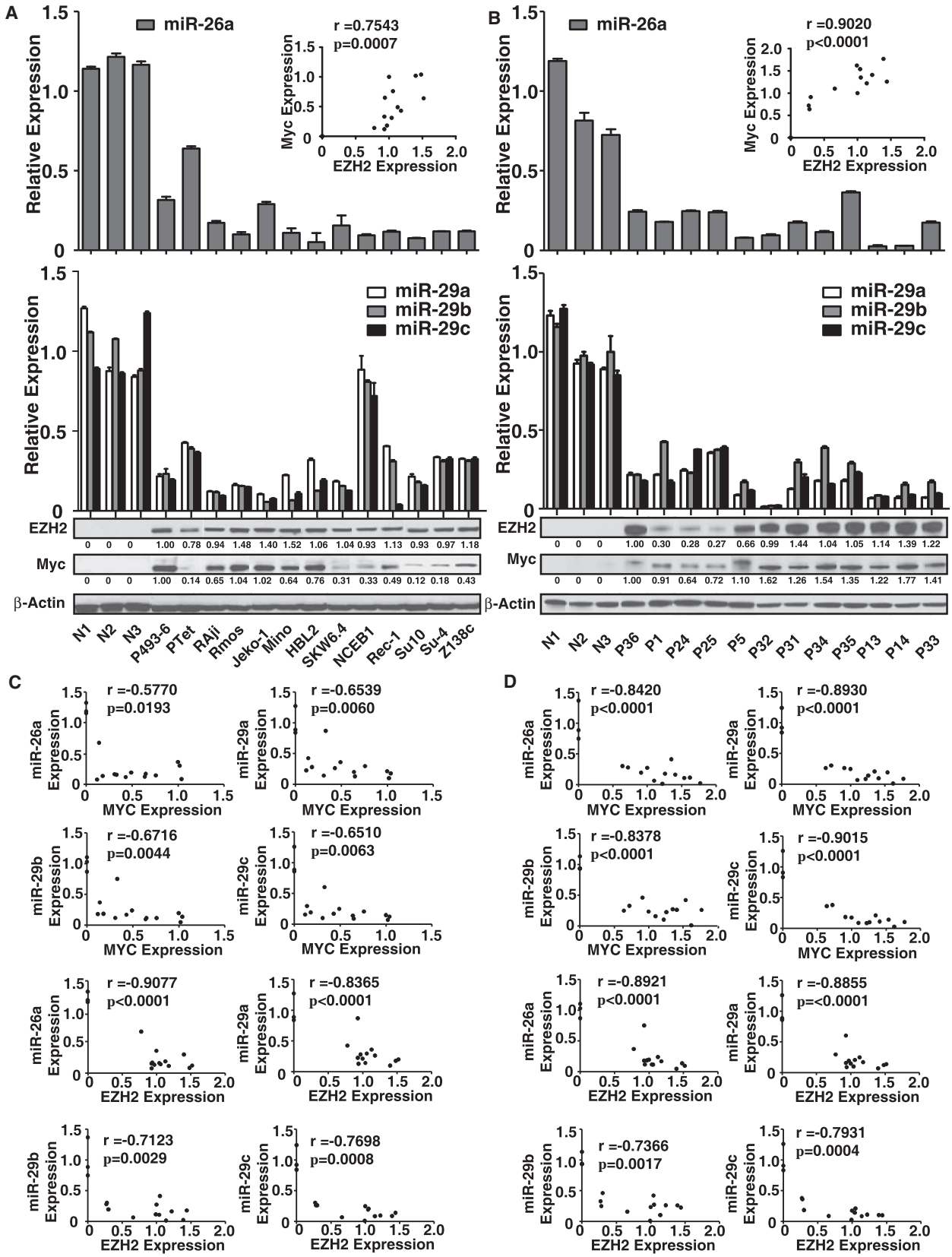
A
B
C
D
miR-26a
r =0.7543
p=0.0007
r =0.9020
p<0.0001
Relative Expression
Myc Expression
EZH2 Expression
miR-29a
miR-29b
miR-29c
EZH2
Myc
β-Actin
N1 N2 N3 P493-6 PTet RAji Rmos Jeko-1 Mino HBL2 SKW6.4 NCEB1 Rec-1 Su10 Su-4 Z138c
N1 N2 N3 P36 P1 P24 P25 P5 P32 P31 P34 P35 P13 P14 P33
MYC Expression
r =-0.5770
p=0.0193
r =-0.6539
p=0.0060
r =-0.6716
p=0.0044
r =-0.6510
p=0.0063
r =-0.9077
p<0.0001
r =-0.8365
p<0.0001
r =-0.7123
p=0.0029
r =-0.7698
p=0.0008
r =-0.8420
p<0.0001
r =-0.8930
p<0.0001
r =-0.8378
p<0.0001
r =-0.9015
p<0.0001
r =-0.8921
p<0.0001
r =-0.8855
p=<0.0001
r =-0.7366
p=0.0017
r =-0.7931
p=0.0004

thus revealing mechanistic links between EZH2 and its upstream and downstream signaling in MYC-associated lymphomas.

The results on EZH2 regulation of MYC are in agreement with previous studies showing that EZH2 induced MYC expression and provide insight into the mechanisms of MYC activation and EZH2-driven cell proliferation. Recent studies have revealed recurrent somatic mutations of *EZH2* in lymphomas and the inactivating somatic mutations of the H3K27 demethylase, *UTX*, in multiple cancers (van Haaften et al., 2009). These findings suggest that deregulation of H3K27 methylation may also contribute to constitutive MYC activation in these lymphomas and EZH2 trimethylase as an ideal therapeutic target for lymphoma therapy. Here, we reveal that dynamic forces act through a feedback circuit to modulate oncogenic expression of proteins, MYC and EZH2, at the posttranscriptional level via miRNAs. This reverberating relationship ensures the signal transduction of the upstream triggering events, leading to the sustained induction of MYC and EZH2 as well as the suppression of the downstream miR-29 family. Given the role of EZH2 in MYC activation and miR-29 repression, inhibition of EZH2 will target both upstream (MYC) and downstream (miR-29, CDK6, IGF-1R) signaling events of aggressive lymphomas.

The transcriptional and posttranscriptional repression of miRNAs through MYC, HDAC3, and PRC2 could be a common feature of many tumor suppressor miRNAs. Thus, our findings provide rational to redirect therapeutic effort by reactivating these tumor suppressor miRNAs through combined inhibition of HDAC and PRC2. Convincingly, we demonstrated that the combination of HDAC and EZH2 inhibitors (vorinostat and DZNep) or their siRNAs induced more miR-29a/b1 and miR-29b2/c gene expression, resulting in the synergistic reduction of protein levels of CDK6 and IGF-1R and subsequent inhibition of cell survival and colony formation in vitro. Of note, HDAC3 and EZH2 overexpression was detected in essentially all of the lymphoma cell lines and primary samples that we tested, but not in normal B lymphocytes and nontransformed B lymphocytes. This provides a strong rationale that targeting HDAC3 and EZH2 may be more effective in lymphoma cells than in normal B lymphocytes. Indeed, our study showed that vorinostat and DZNep dramatically inhibited cell growth of transformed P493-6 cells and had no or minimal effect on nontransformed P493-6 cells. Finally, in vivo studies presented in this work illustrated that, compared with treatment with each agent alone, combined treatment with DZNep and vorinostat inhibits tumor growth and significantly improves survival of NOD/SCID mice bearing MCL xenografts. These results strongly support further development and testing of a combination of anti-EZH2 and a specific HDAC3 inhibitor against aggressive lymphomas.

EXPERIMENTAL PROCEDURES

Cell Lines, Cell Proliferation, Colony Formation Assay, and Patient Samples

Cell lines and patient sample information are detailed in Supplemental Experimental Procedures. All patient tissue specimens were from fresh biopsy-derived lymphoma tissues (lymph nodes) after informed consent was obtained, in accordance with the Declaration of Helsinki and after approval by the Institutional Review Board of the University of South Florida.

Details of cell proliferation and colony formation assays are also described in the Supplemental Experimental Procedures.

Co-IP and ChIP

For co-IP in 293T, cells were transfected with plasmids using Lipofectamine 2000 (Invitrogen). Cells were harvested 36 hr after transfection. Protein (200 μg) was immunoprecipitated with the primary antibody (2 μg) overnight at 4°C, and the immunocomplexes were resolved by SDS-PAGE followed by immunoblot analysis.

For endogenous protein interaction in Jeko-1, IP was performed using the Pierce Co-IP Kit (Thermo Scientific). Six micrograms of anti-HDAC3 antibody, anti-SUZ12 antibody, or normal rabbit immunoglobulin G (IgG) was coupled to AminoLink Plus Coupling Resin according to the manufacturer's protocol. Immune complexes were eluted from the resin and analyzed by SDS-PAGE followed by immunoblot analysis.

For P493-6 cell line, cells were lysed in NP-40 lysis buffer. Protein (1,000 μg) was immunoprecipitated with the primary antibody (2 μg) overnight at 4°C. HDAC3 was detected using GenScript One-Hour IP-Western Kits.

For the ChIP assay, 2×10^6 cells and 3 μg of antibody was used per IP. The immunoprecipitated DNA was treated with RNase (Ambion) for 30 min at 37°C and proteinase K (Roche) for an hour at 45°C.The DNA was purified with QIAGEN PCR Spin columns. Purified DNA was analyzed by real-time PCR using specific primers. Primer sequences used in ChIP assay are listed in the Supplemental Experimental Procedures.

Luciferase Assays

Cells transfected with indicated plasmid were harvested and subjected to luciferase reporter assay using the luciferase assay system according to the manufacturer's instructions (Promega). Details of this analysis and procedure are described in the Supplemental Experimental Procedures.

siRNA Knockdown and Short-Hairpin RNA-Mediated Gene Knockdown

For transient trasfection of siRNA, 5×10^6 cells were transfected by electroporation using Nucleofector (Amaxa) according to the manufacturer's instruction.

For short-hairpin RNA-mediated gene knockdown, cells were transduced with indicated lentivirus particles followed with puromycin selection. The knockdown efficiency was confirmed by western blot.

Figure 7. miR-26a and miR-29 Downregulation Are Reversely Correlated with Upregulation of MYC and EZH2 in MCL and Other Aggressive MYC-Expressing Lymphomas

(A) miR-26a and miR-29 expression levels and MYC and EZH2 protein levels in MCL and other aggressive B-cell lymphoma cell lines. Cell lines were as follows: Jeko-1, Mino, HBL-2, NCEB-1, REC-1, Z138c (MCL); Raji and Ramos (Burkitt lymphoma) SUDHL-4 (Su-4), SUDHL-10 (Su10) (transformed large B-cell lymphoma); and SKW6.2 (EBV-associated lymphoma).

(B) miR-26a and miR-29 expression levels and MYC and EZH2 protein levels in primary MCL samples and other aggressive B-cell lymphoma samples. Samples were as follows: P1 and P5 (aggressive MCL); P13 and P31–P35 (Burkitt lymphoma); P14, P24, P25, and P36, (high-grade transformed diffuse large B-cell lymphomas). N1–N3, CD19 sorted normal B lymphocytes. miR-26a and miR-29 expression levels were measured by qRT-PCR and normalized to RNU44. MYC and EZH2 expression levels were evaluated by western blot; in (A) and (B), the relative levels of MYC and EZH2 protein were measured by quantitative densitometry and are indicated below each lane. Insert, correlation between MYC and EZH2 protein. r, correlation coefficient.

(C) Correlation between MYC/EZH2 protein expressions with miR-26a/miR-29a-c level in MCL and other aggressive B-cell lymphoma cell lines. r, correlation coefficient.

(D) Correlation between MYC/EZH2 protein expressions with miR-26a/miR-29a-c level in primary MCL and other aggressive B-cell lymphoma samples. r, correlation coefficient. Results are representative of three independent experiments or means ± SD from at least three biological replicates.

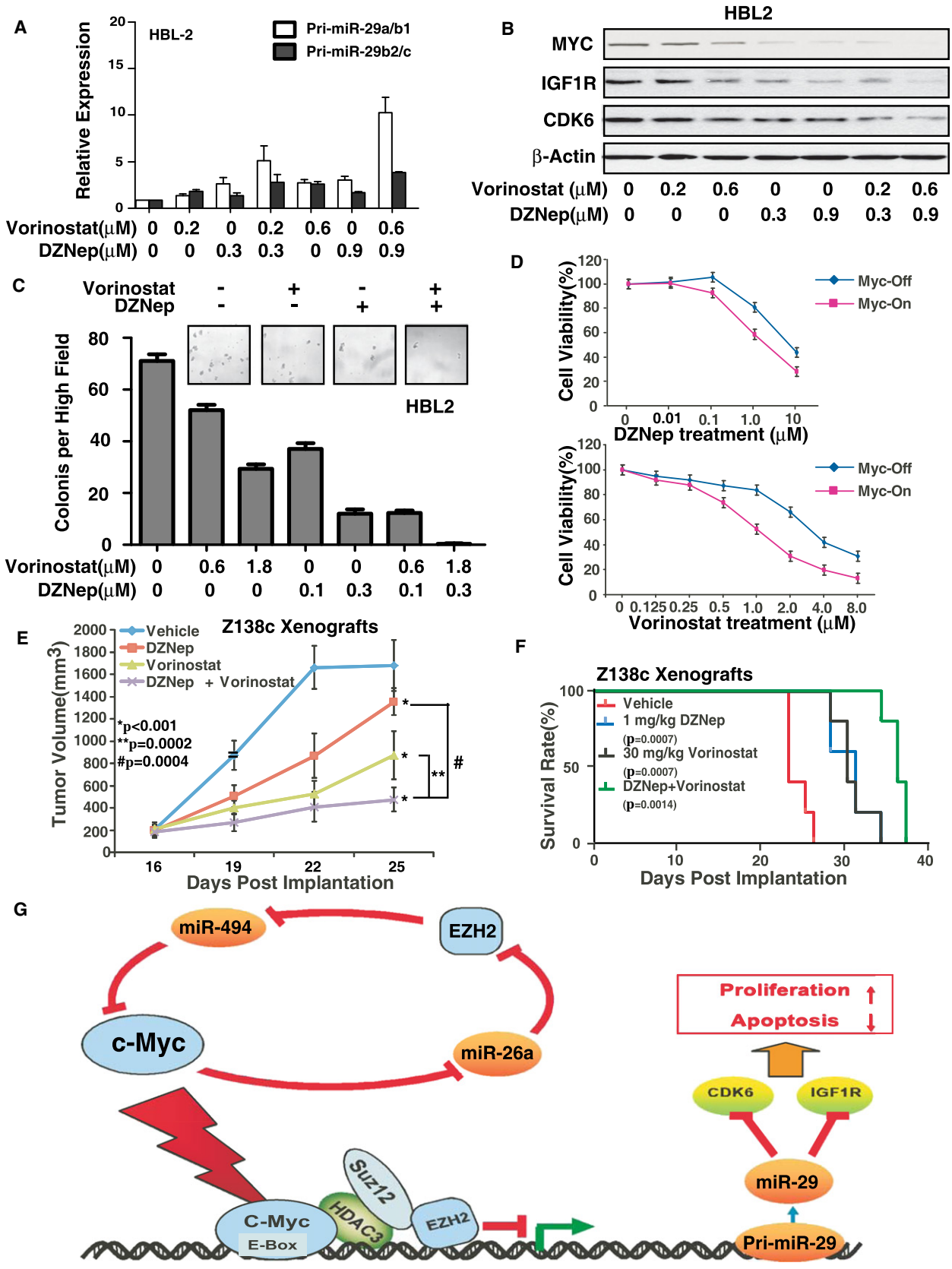
A
HBL-2
Pri-miR-29a/b1
Pri-miR-29b2/c
Relative Expression
Vorinostat(μM) 0 0.2 0 0.2 0.6 0 0.6
DZNep(μM) 0 0 0.3 0.3 0 0.9 0.9
B
HBL2
MYC
IGF1R
CDK6
β-Actin
Vorinostat (μM) 0 0.2 0.6 0 0 0.2 0.6
DZNep(μM) 0 0 0 0.3 0.9 0.3 0.9
C
Vorinostat - + - +
DZNep - - + +
HBL2
Colonis per High Field
Vorinostat(μM) 0 0.6 1.8 0 0 0.6 1.8
DZNep(μM) 0 0 0 0.1 0.3 0.1 0.3
D
Cell Viability(%)
Myc-Off
Myc-On
DZNep treatment (μM)
Vorinostat treatment (μM)
E
Z138c Xenografts
Vehicle
DZNep
Vorinostat
DZNep + Vorinostat
*p<0.001
**p=0.0002
#p=0.0004
Tumor Volume(mm3)
Days Post Implantation
F
Z138c Xenografts
Vehicle
1 mg/kg DZNep
(p=0.0007)
30 mg/kg Vorinostat
(p=0.0007)
DZNep+Vorinostat
(p=0.0014)
Survival Rate(%)
Days Post Implantation
G
miR-494
EZH2
c-Myc
miR-26a
Proliferation
Apoptosis
CDK6
IGF1R
miR-29
Pri-miR-29
C-Myc
E-Box
HDAC3
Suz12
EZH2

The details of these analysis and procedures are described in the Supplemental Experimental Procedures.

qRT-PCR Analysis and miRNA Microarray Analysis

For qRT-PCR analysis, total RNA was isolated from cells with Trizol reagent (Invitrogen). qRT-PCR was performed according to the manufacturer's instructions (Applied Biosystems).

Jeko-1 cells were treated with DZNep for 72 hr. Total RNA was extracted and reverse transcribed into cDNA using the Megaplex Primer Pools by TaqMan miRNA reverse transcription kit (Applied Biosystems). The cDNAs were used to perform the microarray analysis using TaqMan Array miRNA Cards according to the manufacturer's instructions. Array data were analyzed using DataAssist Software V3.0 (Applied Biosystems).

Tumorigenesis Assays

Z138c cells (5×10^6) were injected into flanks of NOD/SCID mice (n = 6 mice per condition). Treatment was initiated when mean tumor volume was approximately 200 mm^3. Mice were treated intraperitoneally with dimethyl sulfoxide (DMSO) (vehicle), 1 mg/kg of DZNep twice per week, and/or 30 mg/kg of Vorinostat daily for 2 weeks. Tumor growth was measured by calipers every 3 days. Survival of the mice in all groups is represented by Kaplan-Meier plot. All animal studies were performed in accordance with the Kansas University Cancer Center Institutional Guidelines and Regulations for animal care and under protocols approved by the Kansas University Medical Center Institutional Animal Care and Use Committee.

Statistical Analysis

All of the analyses were completed with SPSS 11.0 software, with $p < 0.05$ considered statistically significant. Statistical analysis for cell proliferation and tumor growth curve was carried out by an analysis of variance. A log-rank (Mantel-Cox) test was used to test the Kaplan-Meier plot.

ACCESSION NUMBERS

The GEO database accession number for the microarray data is GSE40019.

SUPPLEMENTAL INFORMATION

Supplemental Information includes six figures and Supplemental Experimental Procedures and can be found in this article online at http://dx.doi.org/10.1016/j.ccr.2012.09.003.

ACKNOWLEDGMENTS

We are grateful to the Tissue Procurement and Molecular Core Laboratory at Moffitt Cancer Center for providing specimens and molecular analysis. We thank Rasa Hamilton for editorial assistance. This work was supported by grants from the National Cancer Institute (Grant R01 CA137123 to J.T.), the Maher Fund (to J.T.), the Susan and John Sykes Lymphoma Research Fund (to J.T.) and the Lymphoma Research Foundation (to J.T.).

Received: November 22, 2011
Revised: March 30, 2012
Accepted: September 4, 2012
Published: October 15, 2012

REFERENCES

Chang, T.C., Yu, D., Lee, Y.S., Wentzel, E.A., Arking, D.E., West, K.M., Dang, C.V., Thomas-Tikhonenko, A., and Mendell, J.T. (2008). Widespread microRNA repression by Myc contributes to tumorigenesis. Nat. Genet. *40*, 43–50.

Chen, H., Tu, S.W., and Hsieh, J.T. (2005). Down-regulation of human DAB2IP gene expression mediated by polycomb Ezh2 complex and histone deacetylase in prostate cancer. J. Biol. Chem. *280*, 22437–22444.

Dave, S.S., Fu, K., Wright, G.W., Lam, L.T., Kluin, P., Boerma, E.J., Greiner, T.C., Weisenburger, D.D., Rosenwald, A., Ott, G., et al; Lymphoma/Leukemia Molecular Profiling Project. (2006). Molecular diagnosis of Burkitt's lymphoma. N. Engl. J. Med. *354*, 2431–2442.

Fabbri, M., Garzon, R., Cimmino, A., Liu, Z., Zanesi, N., Callegari, E., Liu, S., Alder, H., Costinean, S., Fernandez-Cymering, C., et al. (2007). MicroRNA-29 family reverts aberrant methylation in lung cancer by targeting DNA methyltransferases 3A and 3B. Proc. Natl. Acad. Sci. USA *104*, 15805–15810.

Fabbri, M., and Croce, C.M. (2011). Role of microRNAs in lymphoid biology and disease. Curr. Opin. Hematol. *18*, 266–272.

Fiskus, W., Wang, Y., Sreekumar, A., Buckley, K.M., Shi, H., Jillella, A., Ustun, C., Rao, R., Fernandez, P., Chen, J., et al. (2009). Combined epigenetic therapy with the histone methyltransferase EZH2 inhibitor 3-deazaneplanocin A and the histone deacetylase inhibitor panobinostat against human AML cells. Blood *114*, 2733–2743.

Hartmann, E., Fernàndez, V., Moreno, V., Valls, J., Hernández, L., Bosch, F., Abrisqueta, P., Klapper, W., Dreyling, M., Hoster, E., et al. (2008). Five-gene model to predict survival in mantle-cell lymphoma using frozen or formalin-fixed, paraffin-embedded tissue. J. Clin. Oncol. *26*, 4966–4972.

Kota, J., Chivukula, R.R., O'Donnell, K.A., Wentzel, E.A., Montgomery, C.L., Hwang, H.W., Chang, T.C., Vivekanandan, P., Torbenson, M., Clark, K.R., et al. (2009). Therapeutic microRNA delivery suppresses tumorigenesis in a murine liver cancer model. Cell *137*, 1005–1017.

Kurland, J.F., and Tansey, W.P. (2008). Myc-mediated transcriptional repression by recruitment of histone deacetylase. Cancer Res. *68*, 3624–3629.

Liu, S., Wu, L.C., Pang, J., Santhanam, R., Schwind, S., Wu, Y.Z., Hickey, C.J., Yu, J., Becker, H., Maharry, K., et al. (2010). Sp1/NFkappaB/HDAC/miR-29b regulatory network in KIT-driven myeloid leukemia. Cancer Cell *17*, 333–347.

Lu, J., He, M.L., Wang, L., Chen, Y., Liu, X., Dong, Q., Chen, Y.C., Peng, Y., Yao, K.T., Kung, H.F., and Li, X.P. (2011). MiR-26a inhibits cell growth and tumorigenesis of nasopharyngeal carcinoma through repression of EZH2. Cancer Res. *71*, 225–233.

Mott, J.L., Kobayashi, S., Bronk, S.F., and Gores, G.J. (2007). mir-29 regulates Mcl-1 protein expression and apoptosis. Oncogene *26*, 6133–6140.

Figure 8. Combined Inhibition of HDAC and PRC2 Cooperatively Reactivates miR-29 Level and Suppresses Tumor Cell Growth In Vitro and In Vivo

(A) Combined treatment with vorinostat and DZNep induces a higher expression of primary miR-29a/b1, primary miR-29b2/c, and mature miR-29a-c than each agent alone in HBL-2 cells.

(B and C) Combined treatment with vorinostat and DZNep induced higher (B) downregulation of IGF-1R and CDK6 protein and (C) inhibition of clonogenic growth than each agent alone in HBL-2 cells.

(D) Cell proliferation assay (CCK8) showing that MYC-on P493-6 cells are more sensitive than MYC-off P496-3 cells to DZNep and vorinostat treatment.

(E and F) Cotreatment with DZNep and vorinostat inhibits tumor growth and significantly improves survival of NOD/SCID mice bearing MCL xenografts. Tumor growth was measured by calipers. Results are mean tumor volume ± SEM, (treatment versus vehicle control, *$p < 0.001$; combination versus single agent, **$p = 0.0002$; #$p = 0.0004$). Survival of mice in all groups is represented by a Kaplan-Meier plot, and a log-rank test was used (n = 6 mice per condition).

(G) Model of feed-forward regulatory circuit in which MYC contributes to the upregulation of EZH2 via repressing EZH2-targeting miR-26a and that EZH2 in turn relieves MYC negative regulation via MYC-targeting miR-494, thereby generating a positive feedback loop to ensure persistently high protein levels of MYC and EZH2 and further repression of miR-29. Results are representative of three independent experiments or means ± SD from at least three biological replicates. See also Figure S6.

Nilsson, J.A., and Cleveland, J.L. (2003). Myc pathways provoking cell suicide and cancer. Oncogene *22*, 9007–9021.

Pekarsky, Y., Santanam, U., Cimmino, A., Palamarchuk, A., Efanov, A., Maximov, V., Volinia, S., Alder, H., Liu, C.G., Rassenti, L., et al. (2006). Tcl1 expression in chronic lymphocytic leukemia is regulated by miR-29 and miR-181. Cancer Res. *66*, 11590–11593.

Sander, S., Bullinger, L., Klapproth, K., Fiedler, K., Kestler, H.A., Barth, T.F., Möller, P., Stilgenbauer, S., Pollack, J.R., and Wirth, T. (2008). MYC stimulates EZH2 expression by repression of its negative regulator miR-26a. Blood *112*, 4202–4212.

Slack, G.W., and Gascoyne, R.D. (2011). MYC and aggressive B-cell lymphomas. Adv. Anat. Pathol. *18*, 219–228.

So, A.Y., Jung, J.W., Lee, S., Kim, H.S., and Kang, K.S. (2011). DNA methyltransferase controls stem cell aging by regulating BMI1 and EZH2 through microRNAs. PLoS One *6*, e19503.

Sparmann, A., and van Lohuizen, M. (2006). Polycomb silencers control cell fate, development and cancer. Nat. Rev. Cancer *6*, 846–856.

van Haaften, G., Dalgliesh, G.L., Davies, H., Chen, L., Bignell, G., Greenman, C., Edkins, S., Hardy, C., O'Meara, S., Teague, J., et al. (2009). Somatic mutations of the histone H3K27 demethylase gene UTX in human cancer. Nat. Genet. *41*, 521–523.

van Kemenade, F.J., Raaphorst, F.M., Blokzijl, T., Fieret, E., Hamer, K.M., Satijn, D.P., Otte, A.P., and Meijer, C.J. (2001). Coexpression of BMI-1 and EZH2 polycomb-group proteins is associated with cycling cells and degree of malignancy in B-cell non-Hodgkin lymphoma. Blood *97*, 3896–3901.

Visser, H.P., Gunster, M.J., Kluin-Nelemans, H.C., Manders, E.M., Raaphorst, F.M., Meijer, C.J., Willemze, R., and Otte, A.P. (2001). The Polycomb group protein EZH2 is upregulated in proliferating, cultured human mantle cell lymphoma. Br. J. Haematol. *112*, 950–958.

Zhang, X., Chen, X., Lin, J., Lwin, T., Wright, G., Moscinski, L.C., Dalton, W.S., Seto, E., Wright, K., Sotomayor, E., and Tao, J. (2012). Myc represses miR-15a/miR-16-1 expression through recruitment of HDAC3 in mantle cell and other non-Hodgkin B-cell lymphomas. Oncogene *31*, 3002–3008.

Zhao, J.J., Lin, J., Lwin, T., Yang, H., Guo, J., Kong, W., Dessureault, S., Moscinski, L.C., Rezania, D., Dalton, W.S., et al. (2010). microRNA expression profile and identification of miR-29 as a prognostic marker and pathogenetic factor by targeting CDK6 in mantle cell lymphoma. Blood *115*, 2630–2639.